A Centrality-based Graph Learning Framework

Jiajun Yu[1,2] , **Zhihao Wu**[1] , **Jielong Lu**[1] , **Tianyue Wang**[2,3] , **Haishuai Wang**[1*]

[1]College of Computer Science and Technology, Zhejiang University, China
[2]Shanghai Innovation Institute, Shanghai, China
[3]Innovation Institute for Artificial Intelligence in Medicine,
College of Pharmaceutical Sciences, Zhejiang University, China

Abstract

Graph Neural Networks (GNNs) have become powerful models for both node- and graph-level tasks. While node-level learning focuses on individual nodes and their local structures, graph-level learning encounters challenges in capturing the global properties of graphs. In this paper, we conduct a theoretical and experimental analysis of existing graph-level learning frameworks and find that these frameworks typically adopt a single-view perspective based solely on node degree, which limits their ability to capture comprehensive graph characteristics. To address these issues, we propose a multi-view approach that leverages different types of centrality measures to capture diverse aspects of graph structure. We design an attention-based mechanism to adaptively integrate these multiple views, and use it as a readout function to perform weighted summation of node embeddings, termed as **A**daptive **C**entrality **Read**out (ACRead). ACRead demonstrates enhanced flexibility and effectiveness when integrated with various GNN architectures, outperforming state-of-the-art readout methods, including KerRead and Set Transformer. Additionally, this multi-view centrality approach can serve as a standalone graph-level learning framework without relying on GNNs, referred to as **A**daptive **C**entrality-based **G**raph **L**earning (ACGL), which achieves competitive performance by effectively combining different centrality perspectives.

1 Introduction

Graph Neural Networks (GNNs) [Welling and Kipf, 2017; Yu and Jia, 2024; Yu and Jia, 2023; Wu *et al.*, 2023] are a powerful class of machine learning models specifically designed to work on graph-structured data. Their architecture effectively leverages relationships between nodes, enabling their interactions on graphs, making GNNs well-suited for application in various domains like computer vision [Han *et al.*, 2022; Gao *et al.*, 2020], natural language processing [Meng *et al.*, ; Wu *et al.*, 2021], and biological information [Yu *et al.*, 2025; Koh *et al.*, 2024]. Currently, the most popular GNNs were initially developed to learn node representations, demonstrating outstanding performance on a wide range of node-level tasks. Among these, several notable GNNs have each contributed unique advancements to the field: Graph Convolutional Networks (GCN) [Welling and Kipf, 2017] extended the concept of convolution to graph data, also bridging the gap between spatial and spectral GNNs; Graph Attention Networks (GAT) [Veličković *et al.*, 2018] incorporate attention mechanisms into GNN models, allowing the model to weigh the importance of different neighbors dynamically; GraphSAGE [Hamilton *et al.*, 2017] was designed for more scalable graph learning via sampling nodes' local neighborhood. Unlike node-level learning which targets specific nodes and their local neighborhoods, graph-level learning addresses tasks where the objective is to understand properties of the entire graph. This distinction introduces unique challenges, such as the graph isomorphism problem, and it is inevitable to tackle global structural information and manage varying graph sizes and topologies. Graph-level learning holds significant importance in diverse fields like protein classification [Réau *et al.*, 2023], drug discovery [Koh *et al.*, 2024], molecular property prediction [Stärk *et al.*, 2022]. These applications demonstrate its profound impact on scientific and industrial advancements.

Inspired by the outstanding performance of GNNs in node-level tasks, many recent graph-level learning frameworks have extended GNN architectures with graph pooling or called readout operations [Navarin *et al.*, 2019]. Typically, these frameworks first generate node representation matrices for each graph using GNNs, and then a readout function aggregates these node representations to produce a comprehensive graph-level embedding that encapsulates the global information of the entire graph. A representative model in this domain is the Graph Isomorphism Network (GIN) [Chen *et al.*, 2019], which employs a readout function to aggregate node embeddings into a single graph-level vector, aiming to summarize the entire graph's information. However, this framework of directly combining GNNs with readout functions presents certain limitations. By not thoroughly analyzing the inherent characteristics specific to graph-level learning, such approaches may inadvertently lead to information loss during the aggregation process. For instance, GIN lever-

*Corresponding author: haishuai.wang@zju.edu.cn.

ages the Weisfeiler-Lehman test [Shervashidze *et al.*, 2011] to analyze GNNs' expressive power on graph-level learning but is also constrained by this theory. This existing framework can result in suboptimal performance, as it does not inherently address the complexities unique to graph-level tasks.

In this paper, we step further to explore the essence of existing GNN-based graph-level learning pipelines. Through theoretical analyses, we reveal that current approaches using GNNs paired with common readout functions essentially adopt a single-view perspective based solely on degree-based centrality. To address this limitation, we propose a multi-view approach by introducing different types of graph centrality measures, each capturing distinct and complementary aspects of how nodes contribute to the overall graph structure. These diverse centrality measures provide multiple views of node importance, offering a more comprehensive understanding of the graph than the traditional degree-based single view. Building on this multi-view perspective, we propose a novel method called **A**daptive **C**entrality **R**eadout (ACRead), which employs an attention-based mechanism to adaptively integrate information from multiple centrality views when aggregating node representations into graph-level embeddings. ACRead serves as a novel readout function that can be paired with various GNNs. When compared with other state-of-the-art readout functions, ACRead exhibits impressive performance with a variety of supervised and unsupervised GNN backbones. Moreover, we also propose a new graph-level learning framework named **A**daptive **C**entrality-based **G**raph **L**earning (ACGL) that leverages these multiple centrality views directly. ACGL is both simple and effective, which is demonstrated by comprehensive experiments conducted on real-world datasets. Without relying on traditional GNNs, it achieves superior performance over other baselines by effectively combining different centrality perspectives. The main contributions of our paper are summarized as follows:

- We analyze existing graph-level learning frameworks from a centrality perspective, revealing their limitations in integrating only a single view of node degree.
- We propose a multi-view approach based on adaptive centrality, which can be used as a readout function in conjunction with GNNs and can also constitute a GNN-free graph learning framework.
- Comprehensive experiments demonstrate the superior performance of the proposed method, learning more informative graph embeddings than existing frameworks by incorporating diverse centrality perspectives.

2 Proposed Method

2.1 Notation and Problem Formulation

A graph $\mathcal{G}_i$ has n_i nodes, and its adjacency matrix is denoted by $A_{\mathcal{G}_i} \in \mathbb{R}^{n_i \times n_i}$. The degree matrix of $A_{\mathcal{G}_i}$ is $D_{\mathcal{G}_i} = \text{diag}(d_1, \ldots, d_{n_i}) \in \mathbb{R}^{n_i \times n_i}$. The initial node features of the graph $\mathcal{G}_i$ are represented by $X_{\mathcal{G}_i} \in \mathbb{R}^{n_i \times d}$. $\mathcal{G} = \{\mathcal{G}_1, ..., \mathcal{G}_N\}$ is the graph set. We aim to learn the graph representation vector $z_{\mathcal{G}_i}$ for each graph $\mathcal{G}_i$ to support various downstream tasks.

The general pipeline for graph classification using message passing paradigm [Welling and Kipf, 2017] can be summarized in two steps:

Graph Encoding. GNNs are primarily employed to encode graphs through a series of graph convolutional layers. Each layer operates on a message-passing principle, which involves two key steps for aggregating the neighborhood information of each target node:

$$\mathbf{H}_{\mathcal{G}_i} = \text{GNN}\big(\mathcal{G}_i, \mathbf{X}_{\mathcal{G}_i}\big), \tag{1}$$

where a certain GNN model is adopted here and $\mathbf{H}_{\mathcal{G}_i} \in \mathbb{R}^{n_i \times d_L}$ is the output node representation of graph $\mathcal{G}_i$.

Readout Function. To unify each size of the graph, following the convolution operation performed by the GNNs, the node embedding matrix $\mathbf{H}_{\mathcal{G}i}$ is processed through a readout function. This function transforms $\mathbf{H}_{\mathcal{G}i} \in \mathbb{R}^{n_i \times d_L}$ into a graph vector $\mathbf{z}_{\mathcal{G}i} \in \mathbb{R}^{d_L}$, which is essential for the graph classification task,:

$$\mathbf{z}_{\mathcal{G}_i} = \text{READOUT}\big(\{\mathbf{H}_{\mathcal{G}_i}[j,:] \mid v_j \in \mathcal{G}_i\}\big), \tag{2}$$

where $\mathbf{H}_{\mathcal{G}_i}[j,:]$ denotes the j-th row of the node embedding matrix for graph $\mathcal{G}_i$, i.e., the representation of node v_j, and $\mathbf{H}_{\mathcal{G}_i}[:,j]$ will refer the j-th column of the node representations for graph $\mathcal{G}_i$.

2.2 Revisiting Graph-level Learning Paradigm

The aforementioned two steps represent the most common frameworks in current graph-level learning, demonstrating good performance in related tasks. However, some studies [Garg *et al.*, 2020; Balcilar *et al.*, 2021] have indicated that the expressive capacity of this paradigm has significant limitations. For instance, Chen *et al.* pointed out that this approach is constrained by the Weisfeiler-Lehman test [Shervashidze *et al.*, 2011]. Therefore, we examine the essence of existing graph-level learning frameworks from a new perspective and build a novel pipeline. Although current GNNs are diverse, it has been discovered that similar performance can be achieved by simplifying them and retaining core mechanisms. Therefore, we discuss the streamlined framework. Following the assumptions in [Wu *et al.*, 2019], where the nonlinearity is removed and weights are collapsed, we have the specified graph encoding process formulated as

$$\mathbf{H}_{\mathcal{G}_i} = \text{GNN}\big(\mathcal{G}_i, \mathbf{X}_{\mathcal{G}_i}\big) = \mathbf{U}^k_{\mathcal{G}_i}\mathbf{X}_{\mathcal{G}_i}\mathbf{W}, \tag{3}$$

where $\mathbf{U}_{\mathcal{G}_i}$ is the adjacency matrix, and a k-hop message passing is performed here. Then the readout function is conducted to extract the graph-level representation of each graph. We find that common readout functions can be uniformly described as

$$\mathbf{z}_{\mathcal{G}_i} = \text{READOUT}\big(\{\mathbf{H}_{\mathcal{G}_i}[j,:] \mid v_j \in \mathcal{G}_i\}\big) = \mathbf{r}^\top_{\mathcal{G}_i}\mathbf{H}_{\mathcal{G}_i}, \tag{4}$$

where $\mathbf{r}_{\mathcal{G}_i}$ is defined as a readout vector which is specified by the adopted readout function. Existing GNN-based graph-level learning frameworks follow this process of combining node-level representation learning and graph-level readout. However, this combination is crude, expecting to inherit the excellent performance of GNNs on node-level tasks while ignoring the important question of what information should be

learned for the graph-level prediction. We therefore proceed to analyze the nature of the existing framework and the reasons for its limitations.

Remark 1. The most common readout functions used in graph-level learning can be reformulated as

$$\begin{cases} \mathrm{SUM}(\mathbf{H}_{\mathcal{G}_i})[j] = \mathbf{1}_{\mathcal{G}_i}^\top(\mathbf{H}_{\mathcal{G}_i}[:,j]), \\ \mathrm{MEAN}(\mathbf{H}_{\mathcal{G}_i})[j] = \mathbf{e}_{\mathcal{G}_i}^\top \mathbf{H}_{\mathcal{G}_i}[:,j], \\ \mathrm{MAX}(\mathbf{H}_{\mathcal{G}_i})[j] = [\mathcal{I}_{max}(\mathbf{H}_{\mathcal{G}_i}[:,j])]^\top \mathbf{H}_{\mathcal{G}_i}[:,j], \\ \mathrm{ATTENTION}(\mathbf{H}_{\mathcal{G}_i})[j] = [f_\Omega^{att}(\mathbf{H}_{\mathcal{G}_i})]^\top \mathbf{H}_{\mathcal{G}_i}[:,j], \end{cases} \tag{5}$$

where $\mathbf{1}_{\mathcal{G}_i}$ denotes an all-one vector, $\mathbf{e}_{\mathcal{G}_i} = [1/n_i, \cdots, 1/n_i]$, and $\mathcal{I}_{max}(\mathbf{x})_i = \mathbb{I}\{i = \arg\max(\mathbf{x})\}$. That is, the readout functions can be described as the inner product over the feature dimensions for a node representation and a particular readout vector.

Remark 2. Combining Equations (3), (4), (5) and the above analyses, the pipeline of existing GNN-based graph-level learning can be further written as

$$\begin{aligned} z_{\mathcal{G}_i} &= \mathrm{READOUT}\big(\mathrm{GNN}\big(\mathcal{G}_i, \mathbf{X}_{\mathcal{G}_i}\big)\big) \\ &= \mathbf{r}_{\mathcal{G}_i}^\top\big(\mathbf{U}_{\mathcal{G}_i}^k \mathbf{X}_{\mathcal{G}_i}\mathbf{W}\big) = \mathbf{c}_{\mathcal{G}_i}^\top\big(\mathbf{X}_{\mathcal{G}_i}\mathbf{W}\big), \end{aligned} \tag{6}$$

where $\mathbf{c}_{\mathcal{G}_i} = \big(\mathbf{r}_{\mathcal{G}_i}^\top \mathbf{U}_{\mathcal{G}_i}^k\big)^\top$, which actually computes a certain statistic related to degree for each node. Subsequently, the vector $\mathbf{c}_{\mathcal{G}_i}$ makes a weighted summation of the node features, only depending on this statistic to obtain a representation of the entire graph $\mathcal{G}_i$. Our analysis reveals the nature of the existing framework, which straightforwardly combines powerful GNNs and readout functions, but is essentially just a weighted degree-based summation. This pipeline struggles to exploit the capabilities of GNNs and potentially undermines the performance of downstream tasks.

To be specific, we take SUM as an example, the vector of ones $\mathbf{1}_{\mathcal{G}_i}$ is selected to be the readout vector, then we have

$$\mathbf{z}_{\mathcal{G}_i} = \mathbf{1}_{\mathcal{G}_i}^\top\big(\mathbf{U}_{\mathcal{G}_i}^k \mathbf{X}_{\mathcal{G}_i}\mathbf{W}\big) = \mathbf{c}_{\mathcal{G}_i}^\top\big(\mathbf{X}_{\mathcal{G}_i}\mathbf{W}\big). \tag{7}$$

where the l-th value of $\mathbf{c}_{\mathcal{G}_i}$ is

$$\mathbf{c}_{\mathcal{G}_i}[l] = \mathbf{1}_{\mathcal{G}_i}^\top \mathbf{U}_{\mathcal{G}_i}^k[:,l] \tag{8}$$

Based on these formulations, three well-known message passing strategies are considered:

1. **Message Passing of GIN**: GIN adopts the message passing mechanism with a non-normalized adjacency matrix, i.e., $\mathbf{U}_{\mathcal{G}_i} = \mathbf{A}_{\mathcal{G}_i}$. Therefore each element in $c_{\mathcal{G}_i}$ is calculated as

$$\mathbf{c}_{\mathcal{G}_i}[l] = \sum_j \mathbf{A}_{\mathcal{G}_i}^k[j,l]. \tag{9}$$

2. **Message Passing of GCN (Random Walk):** For the widely used GCN, there are two strategies. One is to adopt random walk normalized adjacency matrix $\mathbf{U}_{\mathcal{G}_i} = \mathbf{A}_{\mathcal{G}_i}\mathbf{D}_{\mathcal{G}_i}^{-1}$, then we have the following vector $\mathbf{c}_{\mathcal{G}_i}$:

$$\mathbf{c}_{\mathcal{G}_i}[l] = \sum_j \left(\frac{\mathbf{A}_{\mathcal{G}_i}[j,l]}{\mathbf{D}_{\mathcal{G}_i}[l,l]}\right)^k, \tag{10}$$

3. **Message Passing of GCN (Symmetric):** The more popular message passing in GCN is with symmetrically normalized adjacency matrix $\mathbf{U}_{\mathcal{G}_i} = \mathbf{D}_{\mathcal{G}_i}^{-\frac{1}{2}}\mathbf{A}_{\mathcal{G}_i}\mathbf{D}_{\mathcal{G}_i}^{-\frac{1}{2}}$:

$$\mathbf{c}_{\mathcal{G}_i}[l] = \sum_j \left(\frac{\mathbf{A}_{\mathcal{G}_i}[j,l]}{\sqrt{\mathbf{D}_{\mathcal{G}_i}[j,j]}\sqrt{\mathbf{D}_{\mathcal{G}_i}[l,l]}}\right)^k, \tag{11}$$

Through the analyses above, we find that the existing graph-level learning pipeline can be viewed as an aggregation of node information based on a certain statistic of all nodes. This statistic, like the node degree here, is used as a basis for integrating node information.

2.3 Adaptive Centrality

It can be seen that existing methods are essentially based on a single statistic–node degree and do not explicitly design the learning mechanism of the overall framework. We first introduce the concept of centrality [Sade, 1989]. The centrality of nodes on a graph describes the importance of nodes in the whole graph, and there are several critical centrality measures beyond the degree-based ones:

Closeness Centrality of a node i is the reciprocal of the average shortest path distance from node i to all other nodes:

$$\mathbf{c}_{clo}[i] = \frac{1}{\sum_{j\neq i} d(i,j)}. \tag{12}$$

$d(i,j)$ is the shortest path distance between nodes i and j.

Betweenness Centrality of a node i is computed by the shortest paths between all pairs of nodes s and t and counting how many of these paths pass through node i:

$$\mathbf{c}_{bet}[i] = \sum_{s\neq i\neq t} \frac{\gamma_{st}(i)}{\gamma_{st}}, \tag{13}$$

where γ_{st} is the number of shortest paths between nodes s and t, and $\gamma_{st}(i)$ is the number of paths through node i.

Bridge Centrality. For an edge (i,j) that is not part of any bridge, node i has a bridge centrality of 1, otherwise 0, i.e.,

$$\mathbf{c}_{bri}[i] = \begin{cases} 1 & \text{if node } i \text{ is not part of any bridge} \\ 0 & \text{otherwise} \end{cases}. \tag{14}$$

Building on the above analyses of the existing graph-level learning paradigm and the concept of centrality, two research questions for further experimental investigation are *(1) whether models based only on centrality are comparable to existing graph-level learning frameworks? (2) how does different centrality affect graph-level learning performance?* To answer these questions, we conducted an experiment on the performance of two common GNN baselines as well as GNN-free baselines based on different centrality. Note that the centrality-based baselines utilize the MLP as a trainable component, and then readout the graph representations by different centrality, respectively. As shown in Fig 1, it is obvious that centrality-based models can achieve comparable or even better performance without the well-known message passing mechanism. This result corroborates our theoretical analysis that a straightforward combination of GNNs and readout

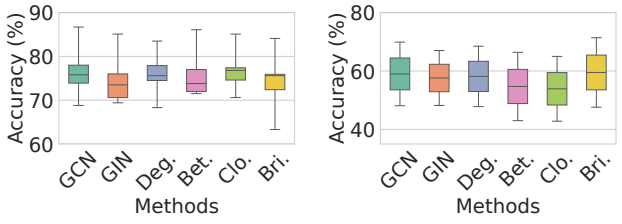

(a) Molecule Dataset (b) Social Network Dataset

Figure 1: The graph classification performance of weight summation using different centrality combinations.

functions collapses into a simple model based on a single type of centrality. In addition, it is observed that a single centrality may not adapt to different types of graph data. These results highlight the importance of selecting appropriate centrality measures based on the nature of the dataset, as they can significantly influence the graph-level tasks.

The results of this experiment inspired us to design a centrality-based framework for graph-level tasks, which touches on the essence more than existing pipelines, but also poses challenges. Since the applicability of different centrality to different types of graph data varies, manually selecting the most appropriate centrality can be very labor-intensive. Thus we would like to learn an adaptive centrality to synthesize the information provided by different centrality.

First, we construct a centrality matrix $\mathbf{C}_{\mathcal{G}_i} \in \mathbb{R}^{n_i \times s}$ collecting various centrality measures for each graph $\mathcal{G}_i$, where s denotes the number of initial centrality measures. Subsequently, a trainable weight vector $\mathbf{w} \in \mathbb{R}^s$ is used to measure the overall importance of each centrality. Specifically, we let each element in $\mathbf{w}$ weight each column in $\mathbf{C}_{\mathcal{G}_i}$, as $\mathbf{C}_{\mathcal{G}_i} = [w[1]C_{\mathcal{G}_i}[:,1], ..., w[s]C_{\mathcal{G}_i}[:,s]]$. This allows the model to initially learn how much information each centrality should provide to the subsequent process. Then we apply normalization to the centrality matrix due to the different scales of the centrality measures, which enhance model stability, i.e., $\hat{\mathbf{C}}_{\mathcal{G}_i} = \frac{\mathbf{C}_{\mathcal{G}_i} - \mu_{\mathcal{G}_i}}{\sigma_{\mathcal{G}_i}}$. This involves calculating the mean $\mu_{\mathcal{G}_i}$ and variance $\sigma_{\mathcal{G}_i}$.

After this, to further extract the information in the centrality matrix as well as the importance of each centrality and the interactions between them, we designed a centrality attention mechanism:

$$\mathbf{\Xi}_{\mathcal{G}_i} = \mathrm{Softmax}\left(\frac{\mathbf{Q}_{\mathcal{G}_i}^\top \mathbf{K}_{\mathcal{G}_i}}{\sqrt{d}}\right)\mathbf{V}_{\mathcal{G}_i}, \tag{15}$$

where $\mathbf{Q}_{\mathcal{G}_i} = \mathbf{W}_q \hat{\mathbf{C}}_{\mathcal{G}_i}$, $\mathbf{K}_{\mathcal{G}_i} = \mathbf{W}_k \hat{\mathbf{C}}_{\mathcal{G}_i}$, $\mathbf{V}_{\mathcal{G}_i} = \mathbf{W}_v \hat{\mathbf{C}}_{\mathcal{G}_i}$, and d is the dimension of the hidden layer. Through this attention-based manner, we can better capture the data distribution among different centralities and effectively learn an adaptive centrality that accommodates various datasets.

In practice, we also employ multi-head self-attention to enhance the model's expressiveness, allowing the model to capture different aspects of node relationships:

$$\mathbf{\Xi}_{\mathcal{G}_i}^h = \mathrm{Softmax}\left(\frac{(\mathbf{Q}_{\mathcal{G}_i}^h)^\top \mathbf{K}_{\mathcal{G}_i}^h}{\sqrt{d_h}}\right)\mathbf{V}_{\mathcal{G}_i}^h, \tag{16}$$

where $\mathbf{Q}_{\mathcal{G}_i}^h = \mathbf{W}_q^h \hat{\mathbf{C}}_{\mathcal{G}_i}$, $\mathbf{K}_{\mathcal{G}_i}^h = \mathbf{W}_k^h \hat{\mathbf{C}}_{\mathcal{G}_i}$, $\mathbf{V}_{\mathcal{G}_i}^h = \mathbf{W}_v^h \hat{\mathbf{C}}_{\mathcal{G}_i}$, and d_h is the dimension for head h. Finally, the outputs from all heads are concatenated and projected through a linear transformation to produce the final adaptive centrality representation:

$$\mathbf{\Xi}_{\mathcal{G}_i} = \mathrm{CONCAT}(\mathbf{\Xi}_{\mathcal{G}_i}^1, \ldots, \mathbf{\Xi}_{\mathcal{G}_i}^H)\mathbf{W}_O, \tag{17}$$

where $\mathbf{W}_O \in \mathbb{R}^{\sum_{i=1}^H d_i \times d}$ is a learnable weight matrix for the output transformation.

The adaptive centrality $\mathbf{\Xi}_{\mathcal{G}_i} \in \mathbb{R}^{n_{\mathcal{G}_i} \times d}$ modulates the importance of nodes in the final representation. The final graph embedding $\mathbf{z}_{\mathcal{G}_i}$ is computed as the weighted sum of the adaptive centrality, expressed as follows:

$$\mathbf{z}_{\mathcal{G}_i} = g_\Psi(\mathbf{\Xi}_{\mathcal{G}_i}, \mathbf{H}_{\mathcal{G}_i}). \tag{18}$$

The choice of $\mathbf{H}_{\mathcal{G}_i}$ offers considerable flexibility. It can be derived from various approaches, such as the node embeddings learned by a GNN or even the initial node feature vectors themselves. The function g_Ψ also provides a flexible mechanism for integrating the learned centrality $\mathbf{\Xi}_{\mathcal{G}_i}$ with node embeddings to produce the final graph embedding. It can take various forms: for instance, it could be a simple linear transformation that directly converts $\mathbf{\Xi}_{\mathcal{G}_i}$ into a vector, which is then used to perform a weighted summation over the node embeddings. Alternatively, it could act as a mapping function that applies the Hadamard product between $\mathbf{\Xi}_{\mathcal{G}_i}$ and $\mathbf{H}_{\mathcal{G}_i}$, followed by a summation.

In summary, the flexibility in the choice of g_Ψ and $\mathbf{H}_{\mathcal{G}_i}$ allows for adapting the centrality-based method to different scenarios, leveraging either learned representations from GNN models or raw feature inputs, depending on the needs of the task or the dataset characteristics. Moreover, our ACGL framework can incorporate other graph learning strategies, making it a highly adaptable and extensible method for a wide range of graph-based tasks.

2.4 Overall Framework

For better understanding, we briefly describe our proposed method in this subsection

$$\begin{cases} \mathbf{H}_{\mathcal{G}_i} = f_{\mathcal{W}}(\mathcal{G}_i, \mathbf{X}_{\mathcal{G}_i}), \\ \mathbf{\Xi}_{\mathcal{G}_i}^h = \mathrm{M}_\Phi(\mathcal{G}_i), \\ \mathbf{z}_{\mathcal{G}_i} = g_\Psi(\mathbf{\Xi}_{\mathcal{G}_i}, \mathbf{H}_{\mathcal{G}_i}), \end{cases} \tag{19}$$

where M_Φ denotes the adaptive centrality learning process, which contains the initial construction of $\mathbf{C}_{\mathcal{G}_i}$, Equations (16) and (17). Φ is the set of all trainable parameters, similarly we have $\mathcal{W}$ and Ψ for corresponding processes. $f_{\mathcal{W}}$ is an encoder chosen from linear layer, MLP, and GNNs. When equipped with GNNs, the model can be viewed as ACRead, while it becomes ACGL when choosing a linear layer or an MLP.

For a comprehensive understanding of computational efficiency, we analyze the time complexity of our proposed method for N graphs. The GNN encoder, responsible for transforming initial node features into node embeddings, exhibits a time complexity of $\mathcal{O}(N(nd + |\mathcal{E}|)(Ld + d_0))$. Here, n denotes the maximum number of nodes, $|\mathcal{E}|$ represents the maximum number of edges, d_0 is the dimension of initial node features, d indicates the maximum hidden dimension,

and L represents the number of GNN layers. This complexity encompasses both propagation and aggregation operations across all layers. In the adaptive centrality mechanism, the query, key, and value mapping layers utilize a hidden dimension d_h (where $d_h \ll d$), resulting in a complexity of $\mathcal{O}(Nnsd_h)$. The attention computations, including score calculations and matrix multiplications, contribute a complexity of $\mathcal{O}(Nhn^2d_h)$ (where $s \ll d_h$ and h represents the number of attention heads). Given that the batch size n remains smaller than the hidden dimension d during training, the overall time complexity maintains at $\mathcal{O}(N(nd + |\mathcal{E}|)(Ld + d_0))$. Notably, the computational overhead introduced by our approach is minimal in the context of the complete framework. For the detailed training times, please refer to Appendix B.5.

3 Expreiments

This section presents experiments to evaluate our proposed methods. We first introduce experimental settings, followed by performance analysis on graph classification and representation learning tasks. We also conduct ablation studies and provide visualizations. Detailed experimental settings are provided in the Appendix B.

3.1 Experiments Setting

Datasets. We utilize 8 graph-level datasets, comprising 2 social network datasets (IMDB-B and IMDB-M) and 6 small-molecule chemical datasets (MUTAG, DD, PROTEINS, NCI1, Mutagenicity and OGBG-Molhiv). All datasets were collected from the TU datasets [Morris *et al.*, 2020] and open graph benchmark repositories [Hu *et al.*, 2020].

Backbone and Baseline. This paper employed six commonly used supervised GNN frameworks: basic GNNs (GCN [Welling and Kipf, 2017], GraphSAGE [Hamilton *et al.*, 2017], SGC [Wu *et al.*, 2019]), and three more expressive GNNs (GAT [Veličković *et al.*, 2018], GIN [Xu *et al.*, 2018], and GUNet [Gao and Ji, 2019]). Besides, two unsupervised GNNs (InfoGraph [Sun *et al.*, 2019] and GraphCL [You *et al.*, 2020]) are also used in this article. Additionally, we selected 11 readout functions as baselines, including simple readouts (Sum, Mean, Max), as well as learnable readouts (Attention [Li *et al.*, 2016], Set2Set [Vinyals *et al.*, 2016], Deep Sets [Zaheer *et al.*, 2017], SRead [Lee *et al.*, 2021], Janossy MLP [Buterez *et al.*, 2022]), sequence-based readouts (Set Transformer, and Janossy GRU [Buterez *et al.*, 2022]), and kernel-based methods (KerRead [Yu *et al.*, 2024]).

Parameter Settings. In this paper, we utilized 9 different centrality measures as the initial centrality features, including: degree centrality, betweenness centrality, closeness centrality, PageRank, hubs, authorities, load centrality, harmonic centrality, and bridge centrality. These centrality measures offer varied insights into node importance and influence within the graph, forming the foundation for our adaptive centrality module. Additional experimental settings and implementation details can be found in the Appendix.

3.2 Experimental Results Analysis

Graph Classification. We conducted a comprehensive graph classification task using 11 readout functions across 6 backbone models. The results for 7 smaller datasets are compared in Tables 1 and Appendix B.4, while the results for a larger dataset are shown in Table 2 to ensure the reliability of our findings. Based on these tables, we observed the following phenomena: (i) ACRead exhibited superior performance, outperforming the previously strongest baseline, KerRead, by an average of 5.1%, 4.2%, and 5.5% on GAT, GUNet, and SGC, respectively. (ii) ACRead demonstrated strong stability. While other readouts performed poorly on GAT and SGC, ACRead maintained consistent performance across all backbones. Specifically, the largest performance difference for ACRead across the 6 backbones was only 3.5%, whereas other readouts showed performance gaps as large as 8.1%. (iii) ACRead's effectiveness persisted even on weaker models. For instance, even on the less expressive SGC model, ACRead outperformed most readouts applied to stronger backbones like GUNet. These results highlight the robustness and effectiveness of ACRead across various models and datasets.

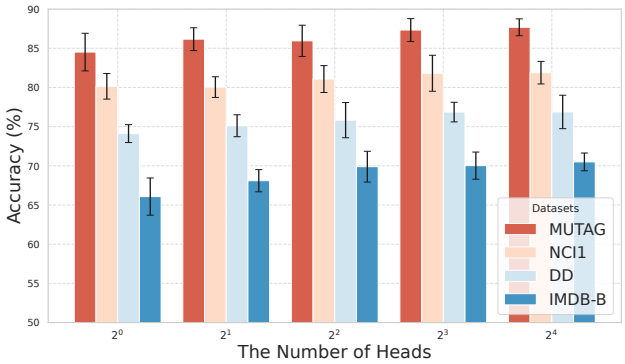

Figure 2: The graph classification performance on four datasets using different numbers of heads.

Graph Representation Learning. The graph clustering results are shown in Table 3, which provides a comparison of 11 readout functions across two unsupervised GNN backbones, InfoGraph and GraphCL, and we can find that: (i) ACRead consistently outperforms other readouts. It achieves the highest performance in terms of both ACC and NMI across multiple datasets, particularly on MUTAG, DD, and NCI1. (ii) ACRead demonstrates strong adaptability across datasets. It maintains robust performance across molecular datasets and social network datasets, confirming its versatility. (iii) While other readouts show significant performance variation depending on the dataset and backbone, ACRead maintains stable results across both InfoGraph and GraphCL. For example, with the InfoGraph backbone, ACRead's NMI ranges from 19.2 to 36.9 across datasets, which is comparatively lower than the fluctuations observed in other methods.

Selection of g_Ψ and $\mathbf{H}_{\mathcal{G}_i}$. To validate the effectiveness of our proposed ACGL framework, we experimented with various configurations of $\mathbf{H}_{\mathcal{G}_i}$ and g_Ψ to assess their performance in graph classification. As shown in Table 4, we conducted experiments on four datasets using three different $\mathbf{H}_{\mathcal{G}_i}$ and two different g_Ψ. The operators $\odot$ and $Linear$ re-

Backbone	Method	MUTAG	DD	PROTEINS	NCI1	Mutagenicity	IMDB-B	IMDB-M	Avg.
GCN [Welling and Kipf, 2017]	Sum	86.7 (5.5)	68.8 (4.7)	73.9 (3.5)	75.8 (2.3)	78.0 (1.8)	69.9 (4.3)	48.1 (4.1)	71.6
	Max	81.8 (9.7)	72.8 (4.3)	66.0 (5.7)	72.4 (3.9)	79.6 (1.7)	71.2 (4.1)	46.7 (4.3)	70.1
	Mean	87.2 (7.3)	71.1 (3.0)	68.1 (4.1)	73.6 (1.8)	78.5 (2.2)	71.1 (3.3)	48.7 (3.8)	71.2
	Set2set	84.0 (4.2)	74.2 (4.9)	72.5 (4.0)	80.9 (1.9	82.0 (0.9)	69.3 (4.3)	48.5 (3.8)	73.1
	Attention	87.2 (4.4)	71.4 (4.0)	70.5 (3.5)	74.5 (2.6)	80.2 (2.3)	72.0 (4.6)	47.1 (5.5)	71.8
	Deep Sets	84.6 (4.9)	73.6 (3.3)	75.5 (5.3)	76.2 (1.9)	78.2 (1.1)	72.0 (2.9)	48.5 (2.8)	72.7
	SRead	86.1 (5.6)	68.8 (3.2)	74.1 (5.0)	75.8 (2.0)	78.4 (1.9)	70.4 (4.7)	47.6 (3.9)	71.6
	Set Transformer	84.6 (6.0)	69.7 (3.9)	71.7 (5.8)	80.7 (2.6)	82.0 (1.7)	72.1 (3.0)	48.3 (1.7)	72.7
	Janossy MLP	76.7 (11.4)	54.0 (3.4)	65.6 (4.0)	71.8 (2.1)	74.6 (1.7)	67.8 (3.3)	48.3 (3.1)	65.5
	Janossy GRU	84.6 (7.7)	58.6 (0.4)	59.5 (0.2)	80.2 (1.6)	73.5 (10.8)	69.3 (3.6)	46.1 (6.6)	67.4
	KerRead	88.3 (6.1)	77.8 (3.0)	75.9 (2.8)	82.6 (2.0)	**82.6 (2.0)**	72.5 (2.4)	49.0 (2.9)	75.5
	ACRead	**89.9 (6.9)**	**78.2 (4.6)**	**76.1 (5.3)**	**83.2 (2.3)**	82.0 (2.6)	**72.9 (5.2)**	**49.7 (4.8)**	**76.0**
GAT [Veličković *et al.*, 2018]	Sum	76.0 (8.8)	73.6 (3.9)	73.6 (3.1)	70.9 (3.0)	75.0 (2.1)	50.0 (0.0)	34.7 (2.3)	64.8
	Max	75.5 (8.4)	74.3 (4.1)	66.9 (5.0)	62.0 (3.5)	73.3 (2.9)	50.0 (0.0)	33.3 (0.0)	62.2
	Mean	74.9 (9.7)	70.3 (4.2)	70.0 (5.4)	69.1 (2.2)	75.8 (2.6)	50.0 (0.0)	33.7 (1.4)	63.4
	Set2set	76.0 (10.9)	75.2 (5.4)	72.6 (4.1)	73.5 (1.6)	78.7 (2.4)	50.0 (0.0)	33.3 (0.0)	65.6
	Attention	78.7 (8.1)	67.7 (4.2)	71.4 (5.4)	69.5 (2.2)	76.9 (1.8)	50.0 (0.0)	33.3 (0.0)	63.9
	Deep Sets	74.0 (12.0)	72.8 (4.6)	74.2 (4.9)	72.0 (1.7)	74.7 (1.3)	50.0 (0.0)	33.3 (0.0)	64.4
	SRead	74.4 (7.8)	70.0 (4.5)	73.8 (4.0)	70.2 (3.1)	74.1 (1.8)	50.2 (0.6)	34.4 (2.3)	63.9
	Set Transformer	74.0 (8.6)	66.8 (4.0)	73.4 (5.2)	72.9 (2.3)	79.6 (1.8)	50.0 (0.0)	33.3 (0.0)	64.3
	Janossy MLP	74.4 (7.4)	52.3 (3.9)	65.0 (4.7)	68.4 (1.8)	71.4 (1.7)	50.0 (0.0)	33.3 (0.0)	59.3
	Janossy GRU	75.5 (9.1)	69.9 (5.0)	59.5 (0.3)	75.5 (3.1)	65.3 (11.2)	50.0 (0.0)	33.3 (0.0)	62.7
	KerRead	79.1 (8.4)	76.4 (4.5)	**77.4 (3.5)**	76.0 (1.2)	80.2 (1.4)	51.4 (1.5)	34.2 (1.8)	67.4
	ACRead	**88.2 (5.3)**	**76.9 (3.5)**	75.2 (4.1)	**81.2 (2.4)**	**80.5 (2.3)**	**64.9 (4.8)**	**40.3 (3.3)**	**72.5**
GIN [Xu *et al.*, 2018]	Sum	85.1 (5.9)	70.6 (3.7)	69.4 (5.0)	73.5 (1.4)	76.0 (1.5)	67.0 (3.4)	48.2 (3.7)	71.0
	Max	84.4 (5.6)	72.1 (4.1)	66.9 (4.9)	72.6 (2.3)	76.6 (1.2)	67.7 (3.8)	48.1 (4.2)	71.2
	Mean	82.0 (8.6)	73.0 (4.0)	69.4 (5.5)	74.4 (1.8)	76.6 (1.7)	66.7 (3.6)	48.3 (3.9)	70.5
	Set2set	86.1 (5.1)	72.0 (4.7)	73.0 (3.2)	73.9 (2.6)	76.9 (1.4)	67.0 (3.4)	49.1 (4.4)	72.6
	Attention	85.4 (4.2)	72.8 (3.9)	73.5 (4.4)	74.2 (1.9)	77.0 (2.2)	66.7 (3.8)	49.3 (4.0)	72.8
	Deep Sets	87.1 (6.2)	73.9 (4.0)	74.1 (4.3)	75.8 (1.5)	76.9 (1.8)	69.8 (3.2)	49.5 (3.8)	73.5
	SRead	84.4 (7.0)	67.4 (4.3)	73.1 (5.5)	73.8 (2.4)	75.6 (1.6)	66.3 (2.8)	48.5 (3.1)	71.0
	Set Transformer	85.1 (6.9)	70.5 (3.7)	72.4 (3.8)	72.6 (2.4)	78.2 (1.9)	68.2 (3.0)	48.4 (4.6)	72.2
	Janossy MLP	75.6 (9.9)	55.5 (3.5)	64.9 (3.6)	73.6 (2.1)	75.0 (1.8)	65.5 (3.2)	47.4 (5.1)	65.1
	Janossy GRU	82.1 (8.8)	57.4 (2.1)	67.5 (4.8)	72.9 (3.5)	72.8 (3.8)	65.2 (3.5)	47.8 (6.7)	66.8
	KerRead	87.5 (5.2)	**77.9 (4.3)**	76.6 (3.7)	78.2 (2.8)	79.0 (1.5)	70.3 (2.0)	50.0 (4.1)	74.3
	ACRead	**87.8 (5.4)**	76.8 (4.3)	**76.9 (4.6)**	**82.4 (3.2)**	**82.2 (2.3)**	**71.5 (3.5)**	**50.6 (3.4)**	**75.5**

Table 1: Performance comparison of various backbone architectures and readout methods across different datasets. The metrics are reported as average accuracy with standard deviation. The bold values denote the best performances per dataset and underlining highlights the second-best performance. Additional backbone architectures are shown in Appendix B.4

spectively represent the Hadamard product using the learned $\boldsymbol{\Upsilon} \in \mathbf{R}^{n_{\mathcal{G}_i} \times d}$ directly, or a linear transformation into a vector of size $n_{\mathcal{G}_i} \times 1$ followed by weighted summation. We observed the following phenomena: (i) More complex $\mathbf{H}_{\mathcal{G}_i}$ typically leads to better results. Using the initial features $X_{\mathcal{G}_i}$ as the starting vector already yields performance comparable to Table 1. However, it's clear that applying an MLP transformation on $X_{\mathcal{G}_i}$ yields even better results, and the best performance is achieved when $H_{\mathcal{G}_i}$ is learned using GNNs for weighted summation, as evidenced in Tables 1. (ii) The $\odot$ operator outperforms the simple linear summation, as it not only applies weights to each node but also to each dimension, enabling the capture of more information.

The Number of Heads. Figure 2 illustrates the relationship between the number of heads and the accuracy across four datasets. The x-axis represents the number of heads, scaled exponentially (from 2^0 to 2^4), while the y-axis shows the corresponding accuracy for each dataset. In general, accuracy tends to increase with a higher number of heads across all datasets. This trend suggests that increasing the number of attention heads in the model contributes positively to classification performance, reflecting improved representation learning. However, the performance improvement diminishes as the number of heads increases from 2^3 to 2^4. While the initial increase in heads (from 2^0 to 2^3) leads to notable accuracy gains across all datasets, the jump from 2^3 to 2^4 shows a much smaller improvement. This trend suggests that after a certain point, adding more heads yields diminishing returns, possibly because the model reaches a saturation point where further splitting attention no longer substantially enhances the representation learning.

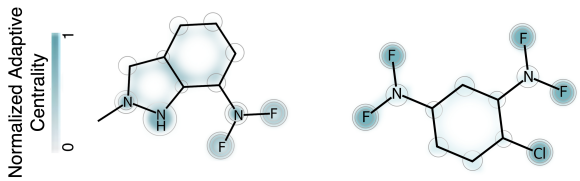

(a) ID 35 (b) ID 82

Figure 3: Visualize the use of adaptive centrality on the MUTAG.

Visiualization. The normalized adaptive centrality scores, scaled between $(0, 1)$, are visualized with darker colors rep-

Dataset	Readout	GCN	GIN	GraphSAGE	GAT	GUNet	SGC	Avg
OGBG-Molhiv # Graphs: 41,127 # Features: 9 # Classes: 2 Avg. # Nodes: 25.5 Avg. # Edges: 27.5	Sum	60.9 (2.9)	71.3 (1.7)	58.3 (2.3)	62.3 (2.1)	59.0 (1.7)	59.7 (2.1)	61.9
	Max	58.4 (2.3)	71.8 (2.0)	66.9 (3.6)	67.7 (2.0)	66.7 (4.4)	66.1 (3.2)	66.3
	Mean	57.4 (1.8)	70.9 (2.4)	51.0 (2.2)	60.4 (2.3)	50.3 (1.0)	50.3 (0.7)	56.7
	Set2set	66.8 (1.8)	70.9 (1.3)	59.4 (1.8)	65.7 (2.0)	56.7 (2.1)	58.0 (1.1)	62.9
	Attention	62.0 (1.7)	70.4 (1.5)	51.1 (1.9)	58.5 (3.0)	51.0 (1.6)	51.8 (2.2)	57.5
	Deep Sets	63.3 (2.0)	52.9 (1.0)	53.1 (0.8)	62.2 (2.2)	53.4 (1.4)	52.7 (1.0)	56.3
	SRead	63.0 (1.4)	70.9 (2.5)	57.2 (1.2)	63.2 (2.9)	59.1 (3.4)	51.8 (2.2)	60.9
	Set Transformer	72.2 (1.6)	71.2 (1.3)	61.3 (1.4)	69.4 (1.5)	61.8 (2.2)	69.2 (2.1)	67.5
	Janossy MLP	52.4 (0.6)	50.0 (0.1)	50.0 (0.1)	51.5 (1.2)	50.0 (0.0)	50.0 (0.0)	50.7
	Janossy GRU	71.1 (1.4)	67.9 (2.6)	68.1 (2.4)	69.1 (1.2)	67.1 (1.9)	68.1 (2.2)	68.6
	KerRead	72.5 (1.6)	72.2 (1.5)	67.1 (1.2)	70.4 (0.7)	67.9 (2.6)	68.9 (2.1)	69.8
	ACRead	**72.9 (1.4)**	**73.1 (1.9)**	**69.2 (1.4)**	**70.6 (1.9)**	**69.5 (1.6)**	**69.4 (1.8)**	**70.6**

Table 2: Graph classification AUC (mean and std%) on OGBG-Molhiv dataset with six GNN backbones, where **bold** denotes the best performance and underlining indicates the second-best performance.

Backbone	Readout	MUTAG		DD		PROTEINS		NCI1		Mutagenicity		IMDB-B		IMDB-M	
		ACC	NMI	ACC	NMI	ACC	NMI	ACC	NMI	ACC	NMI	ACC	NMI	ACC	NMI
InfoGraph [Sun *et al.*, 2019]	Sum	71.3	14.1	59.7	2.6	60.4	2.6	56.6	1.3	56.4	1.7	62.3	4.4	40.8	2.2
	Max	80.9	25.6	60.8	4.7	61.7	2.8	60.4	3.3	57.2	1.6	61.1	4.7	38.9	2.2
	Mean	71.3	14.1	56.5	2.2	62.4	3.4	56.8	1.4	60.0	3.5	63.1	5.2	41.0	2.4
	Set2set	74.5	17.5	63.2	6.0	62.5	3.2	59.0	2.4	62.7	4.3	62.9	5.1	40.5	3.2
	Attention	80.3	24.4	55.2	1.0	59.9	2.4	57.3	1.6	63.3	5.1	62.9	5.0	40.3	1.8
	Deep Sets	76.1	33.5	60.9	3.2	62.3	3.2	57.8	1.9	60.5	3.7	62.4	4.6	41.3	2.2
	SRead	79.3	31.7	60.4	3.6	59.5	2.0	58.3	2.0	61.1	4.2	62.6	4.6	41.5	2.5
	Set Transformer	73.9	16.9	70.3	13.0	59.8	2.6	60.9	3.6	65.2	6.4	63.6	5.4	41.5	1.9
	Janossy MLP	62.8	11.5	55.4	1.3	58.8	0.4	59.4	3.0	62.4	7.3	62.2	4.3	41.9	2.1
	Janossy GRU	70.7	26.0	58.6	0.0	59.4	0.0	58.1	0.0	62.3	0.1	50.1	0.0	42.3	3.5
	KerRead	83.5	36.4	74.8	20.5	63.4	6.3	61.8	3.8	65.7	7.0	63.5	5.3	42.8	2.6
	ACRead	**84.8**	**36.9**	**75.1**	**21.2**	**65.1**	**6.9**	**63.2**	**4.1**	**66.2**	**7.8**	**64.2**	**6.1**	**43.1**	**3.2**
GraphCL [You *et al.*, 2020]	Sum	73.9	16.9	66.0	8.3	64.8	4.7	57.2	1.6	61.5	3.7	57.6	2.4	42.5	3.0
	Max	79.3	21.8	59.1	3.1	64.4	4.5	58.7	2.2	61.1	3.7	62.6	5.0	39.9	3.4
	Mean	73.9	16.9	66.3	8.7	64.4	4.5	55.2	0.8	61.6	3.4	61.6	4.0	42.9	3.3
	Set2set	70.7	17.5	60.7	2.5	63.4	3.2	58.3	2.6	63.6	6.6	64.8	6.4	43.8	3.8
	Attention	76.1	24.3	55.8	0.5	62.0	2.1	57.6	2.3	61.1	3.1	60.9	4.5	39.9	3.5
	Deep Sets	75.0	18.2	58.7	4.1	61.2	2.5	57.8	2.1	64.5	6.2	59.6	3.3	41.8	2.8
	SRead	76.6	24.9	68.1	8.9	65.1	5.0	57.1	2.1	62.2	5.8	63.9	**8.6**	43.9	4.0
	Set Transformer	79.8	32.2	53.7	0.3	58.3	1.7	55.7	1.0	61.4	4.0	59.6	4.2	41.9	2.5
	Janossy MLP	72.3	9.8	52.0	0.2	62.1	2.3	54.3	0.7	64.1	6.0	60.7	3.4	42.3	2.9
	Janossy GRU	81.4	33.8	55.4	0.6	65.1	4.7	56.2	1.2	56.6	1.3	57.7	2.3	44.7	3.0
	KerRead	83.5	34.1	75.4	18.7	70.9	11.2	58.8	2.8	64.2	6.1	64.4	6.5	45.0	3.6
	ACRead	**84.1**	**35.8**	**76.2**	**19.2**	**71.0**	**11.3**	**61.3**	**4.1**	**66.2**	**7.9**	**65.1**	6.9	**46.0**	**4.1**

Table 3: Graph clustering accuracy (ACC) and normalized mutual information (NMI) with two unsupervised GNN backbones (InfoGraph, GraphCL). **Bold** indicates the best performance, and underlining highlights the second-best performance.

$\mathbf{H}_{\mathcal{G}_i}$	g_Ψ	MUTAG	DD	PROTEINS	IMDB-M
$X_{\mathcal{G}_i}$	$\odot$	84.1 (7.2)	75.2 (5.1)	74.1 (4.3)	46.3 (5.2)
$Linear(X_{\mathcal{G}_i})$	$\odot$	86.2 (8.5)	76.2 (5.3)	76.4 (4.5)	48.3 (5.1)
$MLP(X_{\mathcal{G}_i})$	$\odot$	87.7 (8.1)	78.4 (5.8)	76.2 (4.9)	49.3 (4.9)
$X_{\mathcal{G}_i}$	$Linear$	85.1 (7.3)	74.1 (6.2)	75.3 (5.1)	45.9 (3.6)
$Linear(X_{\mathcal{G}_i})$	$Linear$	86.1 (7.2)	75.3 (5.5)	76.1 (4.5)	47.1 (4.9)
$MLP(X_{\mathcal{G}_i})$	$Linear$	87.5 (6.1)	77.5 (5.7)	75.9 (4.6)	48.1 (4.2)

Table 4: The graph classification performance on four datasets using different g_Ψ and $\mathbf{H}_{\mathcal{G}_i}$.

resenting nodes of greater influence on the graph embedding. We randomly selected two samples from the MUTAG dataset, as shown in Figure 3, where the goal is to predict mutagenicity in Salmonella typhimurium. Both samples activate the mutagenic gene. Adaptive centrality identified functional groups like F and Cl as important, while carbon atoms in the benzene ring were less significant. This highlights adaptive centrality's ability to capture node importance, offering insights for future graph-level tasks.

Supplementary Experiment Due to space constraints, additional crucial experiments are included in the appendices, including graph classification performance with GUNet, GraphSAGE, and SGC backbones (Appendix B.4), as well as training time analysis (Appendix B.5).

4 Conclusion

In this paper, we revisited the essence of message passing in graph-level tasks through the perspective of centrality, uncovering that it primarily operates as a weighted summation with degree-based centrality, which represents a single-view of node centrality. Building on this insight, we introduced a novel graph-level learning method with a more generalizable form of centrality–adaptive centrality, which integrates multiple views of node centrality and is utilized to build a novel readout function, called **A**daptive **C**entrality-based **R**eadout (ACRead). ACRead was applied to six supervised and two unsupervised GNN backbones, consistently outperforming existing readout methods across eight graph datasets. Furthermore, the approach could also perform as an individual graph-level learning framework without GNNs, called **A**daptive **C**entrality-based **G**raph **L**earning (ACGL), which still achieved competitive performance by effectively combining different views of node centrality.

Acknowledgements

This work was supported by the National Natural Science Foundation of China (Grant Nos. 62202422 and 62372408).

Contribution Statement

Jiajun Yu and Zhihao Wu contributed equally as co-first authors.

References

[Balcilar *et al.*, 2021] Muhammet Balcilar, Pierre Héroux, Benoit Gauzere, Pascal Vasseur, Sébastien Adam, and Paul Honeine. Breaking the limits of message passing graph neural networks. In *International Conference on Machine Learning*, pages 599–608. PMLR, 2021.

[Buterez *et al.*, 2022] David Buterez, Jon Paul Janet, Steven J Kiddle, Dino Oglic, and Pietro Liò. Graph neural networks with adaptive readouts. In *NeurIPS*, pages 19746–19758, 2022.

[Chen *et al.*, 2019] Ting Chen, Song Bian, and Yizhou Sun. Are powerful graph neural nets necessary? a dissection on graph classification. *arXiv preprint arXiv:1905.04579*, 2019.

[Gao and Ji, 2019] Hongyang Gao and Shuiwang Ji. Graph u-nets. In *ICML*, pages 2083–2092, 2019.

[Gao *et al.*, 2020] Difei Gao, Ke Li, Ruiping Wang, Shiguang Shan, and Xilin Chen. Multi-modal graph neural network for joint reasoning on vision and scene text. In *Proceedings of the IEEE/CVF conference on computer vision and pattern recognition*, pages 12746–12756, 2020.

[Garg *et al.*, 2020] Vikas Garg, Stefanie Jegelka, and Tommi Jaakkola. Generalization and representational limits of graph neural networks. In *International Conference on Machine Learning*, pages 3419–3430. PMLR, 2020.

[Hamilton *et al.*, 2017] Will Hamilton, Zhitao Ying, and Jure Leskovec. Inductive representation learning on large graphs. In *NeurIPS*, 2017.

[Han *et al.*, 2022] Kai Han, Yunhe Wang, Jianyuan Guo, Yehui Tang, and Enhua Wu. Vision gnn: An image is worth graph of nodes. *Advances in neural information processing systems*, 35:8291–8303, 2022.

[Hu *et al.*, 2020] Weihua Hu, Matthias Fey, Marinka Zitnik, Yuxiao Dong, Hongyu Ren, Bowen Liu, Michele Catasta, and Jure Leskovec. Open graph benchmark: Datasets for machine learning on graphs. *Advances in neural information processing systems*, 33:22118–22133, 2020.

[Koh *et al.*, 2024] Huan Yee Koh, Anh TN Nguyen, Shirui Pan, Lauren T May, and Geoffrey I Webb. Physicochemical graph neural network for learning protein–ligand interaction fingerprints from sequence data. *Nature Machine Intelligence*, pages 1–15, 2024.

[Lee *et al.*, 2021] Dongha Lee, Su Kim, Seonghyeon Lee, Chanyoung Park, and Hwanjo Yu. Learnable structural semantic readout for graph classification. In *ICDM*, pages 1180–1185, 2021.

[Li *et al.*, 2016] Yujia Li, Richard Zemel, Marc Brockschmidt, and Daniel Tarlow. Gated graph sequence neural networks. In *ICLR*, 2016.

[Meng *et al.*,] Yuxian Meng, Shi Zong, Xiaoya Li, Xiaofei Sun, Tianwei Zhang, Fei Wu, and Jiwei Li. Gnn-lm: Language modeling based on global contexts via gnn. In *ICLR 2022 Workshop on Deep Learning on Graphs for Natural Language Processing*.

[Morris *et al.*, 2020] Christopher Morris, Nils M Kriege, Franka Bause, Kristian Kersting, Petra Mutzel, and Marion Neumann. Tudataset: A collection of benchmark datasets for learning with graphs. *arXiv preprint arXiv:2007.08663*, 2020.

[Navarin *et al.*, 2019] Nicolò Navarin, Dinh Van Tran, and Alessandro Sperduti. Universal readout for graph convolutional neural networks. In *IJCNN*, pages 1–7, 2019.

[Réau *et al.*, 2023] Manon Réau, Nicolas Renaud, Li C Xue, and Alexandre MJJ Bonvin. Deeprank-gnn: a graph neural network framework to learn patterns in protein–protein interfaces. *Bioinformatics*, 39(1):btac759, 2023.

[Sade, 1989] Donald Stone Sade. Sociometrics of macaca mulatta iii: N-path centrality in grooming networks. *Social Networks*, 11(3):273–292, 1989.

[Shervashidze *et al.*, 2011] Nino Shervashidze, Pascal Schweitzer, Erik Jan Van Leeuwen, Kurt Mehlhorn, and Karsten M Borgwardt. Weisfeiler-lehman graph kernels. *Journal of Machine Learning Research*, 12(9), 2011.

[Stärk *et al.*, 2022] Hannes Stärk, Dominique Beaini, Gabriele Corso, Prudencio Tossou, Christian Dallago, Stephan Günnemann, and Pietro Liò. 3d infomax improves gnns for molecular property prediction. In *International Conference on Machine Learning*, pages 20479–20502. PMLR, 2022.

[Sun *et al.*, 2019] Fan-Yun Sun, Jordan Hoffman, Vikas Verma, and Jian Tang. Infograph: Unsupervised and semi-supervised graph-level representation learning via mutual information maximization. In *ICLR*, 2019.

[Veličković *et al.*, 2018] Petar Veličković, Guillem Cucurull, Arantxa Casanova, Adriana Romero, Pietro Liò, and Yoshua Bengio. Graph attention networks. In *ICLR*, 2018.

[Vinyals *et al.*, 2016] Oriol Vinyals, Samy Bengio, and Manjunath Kudlur. Order matters: Sequence to sequence for sets. In *ICLR*, 2016.

[Welling and Kipf, 2017] Max Welling and Thomas N Kipf. Semi-supervised classification with graph convolutional networks. In *ICLR*, 2017.

[Wu *et al.*, 2019] Felix Wu, Amauri Souza, Tianyi Zhang, Christopher Fifty, Tao Yu, and Kilian Weinberger. Simplifying graph convolutional networks. In *ICML*, pages 6861–6871, 2019.

[Wu *et al.*, 2021] Lingfei Wu, Yu Chen, Heng Ji, and Bang Liu. Deep learning on graphs for natural language processing. In *Proceedings of the 44th International ACM SIGIR Conference on Research and Development in Information Retrieval*, pages 2651–2653, 2021.

[Wu *et al.*, 2023] Zhihao Wu, Zhao Zhang, and Jicong Fan. Graph convolutional kernel machine versus graph convolutional networks. *Advances in neural information processing systems*, 36:19650–19672, 2023.

[Xu *et al.*, 2018] Keyulu Xu, Weihua Hu, Jure Leskovec, and Stefanie Jegelka. How powerful are graph neural networks? In *ICLR*, 2018.

[You *et al.*, 2020] Yuning You, Tianlong Chen, Yongduo Sui, Ting Chen, Zhangyang Wang, and Yang Shen. Graph contrastive learning with augmentations. In *NeurIPS*, pages 5812–5823, 2020.

[Yu and Jia, 2023] Jiajun Yu and Adele Lu Jia. Mlgal: Multi-level label graph adaptive learning for node clustering in the attributed graph. *Knowledge-Based Systems*, 278:110876, 2023.

[Yu and Jia, 2024] Jiajun Yu and Adele Lu Jia. Agcl: Adaptive graph contrastive learning for graph representation learning. *Neurocomputing*, 566:127019, 2024.

[Yu *et al.*, 2024] Jiajun Yu, Zhihao Wu, Jinyu Cai, Adele Lu Jia, and Jicong Fan. Kernel readout for graph neural networks. In Kate Larson, editor, *Proceedings of the Thirty-Third International Joint Conference on Artificial Intelligence, IJCAI-24*, pages 2505–2514. International Joint Conferences on Artificial Intelligence Organization, 8 2024. Main Track.

[Yu *et al.*, 2025] Jiajun Yu, Yizhen Zheng, Huan Yee Koh, Shirui Pan, Tianyue Wang, and Haishuai Wang. Collaborative expert llms guided multi-objective molecular optimization. *arXiv preprint arXiv:2503.03503*, 2025.

[Zaheer *et al.*, 2017] Manzil Zaheer, Satwik Kottur, Siamak Ravanbakhsh, Barnabas Poczos, Russ R Salakhutdinov, and Alexander J Smola. Deep sets. In *NeurIPS*, 2017.